

Analog simulation of melting in two dimensions

B. Pouligny,* R. Malzbender, P. Ryan,[†] and Noel A. Clark

Condensed Matter Laboratory, Department of Physics, University of Colorado, Boulder, Colorado 80309

(Received 21 February 1990)

We have studied a system of macroscopic steel spheres confined to a hexagonal area on the lower surface of a horizontal parallel-plate capacitor. The spheres interact via repulsive electrostatic forces with each other and with the boundary and are in contact with an artificial thermal bath produced by mechanically agitating the entire apparatus. Translational and bond-orientational order evolve from the boundary inward as the temperature is lowered and appear abruptly and simultaneously in the cell center. This result implies a first-order transition between liquid and solid phases.

Theoretical suggestions that melting in two dimensions (2D) might differ substantially from conventional three-dimensional (3D) melting have motivated a large amount of experimental work on 2D melting during the past ten years. Kosterlitz and Thouless first promoted the idea that melting is the consequence of the proliferation of free dislocations in a harmonic crystal.¹ This idea was subsequently generalized by Halperin, Nelson, and Young (HNY) with a model in which dislocation pairs first unbind into free dislocations, which then unbind into free disclinations.²⁻⁴ An interesting consequence of such a scenario is that melting could occur via two second-order transitions, separated by an intervening hexatic phase characterized by liquidlike short-range positional order but long-range orientational order. The search for the hexatic phase has been conducted in a variety of numerical simulations as well as "real" systems; as a recent review⁵ indicates, these experiments have yielded conflicting results and the 2D melting problem remains a challenging one.

An important aspect of both models and experiments is the nature of the local structure and fluctuations in the crystal, hexatic, and liquid phases. So far only computer simulations and colloidal systems⁶ enable direct study of individual particle motions. In this paper we report an analog simulation which we believe is a useful addition to the arsenal of experimental tools available to study statistical physics in two dimensions, and in particular to study individual particle positions and motions in 2D crystals and liquids. Our system consists of macroscopic steel spheres confined to move in two dimensions and in contact with an artificial thermal bath. These spheres interact only through electrostatic forces and are observed to undergo a distinct transition between ordered and disordered phases as a synthetic temperature is varied. This method builds on previous work on model systems with only hard-disk interactions,^{7,8} systems with attractive potentials,⁹ and work by Blonder,¹⁰ who developed the electrostatic technique to model the equilibrium arrangement of vortex lines in finite ⁴He samples. A diagram of the experiment is shown in Fig. 1. The particles are $\frac{1}{16}$ -inch-diam stainless-steel spheres rolling on the bottom surface of a parallel-plate capacitor. The upper plate is transparent glass coated with indium tin oxide (ITO) and is held at an

adjustable positive voltage relative to the lower plate, which is made of glass coated with chromium. The plates are separated by an $\frac{1}{8}$ -inch-thick spacer, having a hole in the form of a hexagon which defines the boundary of the space available to the spheres. A $\frac{1}{16}$ -inch-diam brass rod is glued to the inner edge of the spacer and is also in contact with the lower conducting surface. The positions of the particles are recorded by a video camera attached to an image-processing computer, which extracts the center-of-mass coordinates of the particles.

When a voltage of several hundred to a few thousand volts is applied across the capacitor, the spheres repel each other and the brass rods at the boundary. For spheres which are small relative to the plate separation and which are not too close together the interaction is primarily dipolar; this can be seen by considering the electrostatic images of the spheres and the upper plate in the lower plate.

An artificial temperature T is provided by causing the cell to translate, its center-of-mass moving in a roughly circular horizontal motion of submillimeter dimension. The cell is mounted on rubber supports and is subjected to a periodic time-dependent horizontal force produced by a magnet which rotates inside a steel can attached to the bottom of the cell (see Fig. 1). The amount of temperature so induced is varied by changing the height of the motor, thus changing the strength of the magnetic coupling between the cell and the rotor. The frequency of the driving motor is stabilized at ~ 30 Hz with a feedback cir-

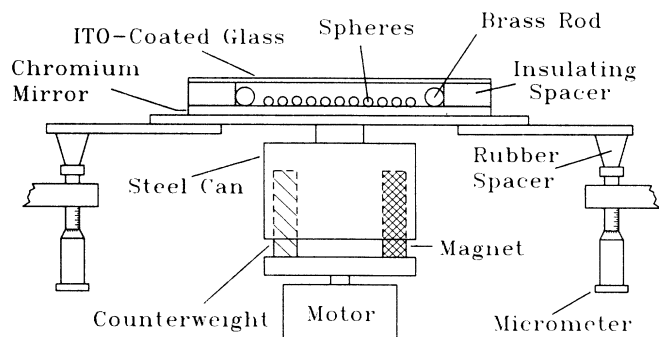


FIG. 1. Diagram of the experimental apparatus.

cuit. Even though the driving force is certainly periodic, the particles respond in a very aperiodic fashion, even when not interacting with other particles. This may be explained by fluctuating forces due to microscopic irregularities of the sphere and lower plate surfaces, including possible particulate contamination.

We have ascertained the nature of the temperature T in our system in two ways. First, we verified that the radial distribution of a single particle in a parabolic potential is Gaussian, using a sphere rolling in a concave lens placed on the cell. The position distribution of the sphere was determined for several different temperatures with the same image analysis procedures used for the actual experiment. The experimental distribution is found to be Gaussian over three decades, as shown in Fig. 2(a). Second, we measured the velocity distribution of individual particles in a 919-particle system by tracking images of the particles from one video frame to the next. The monochrome video frames (512×480 pixel resolution) are digitized by image processing hardware attached to a Sun workstation, recorded at 30 frames/sec on an optical disk, enhanced to remove noise and improve contrast, thresholded to binary (black-white) images, and finally converted to particle coordinates by finding the centroids of the resulting sphere images. The tracking algorithm simply finds the closest sphere in frame $n + 1$ to a sphere in frame n ; this method relies on the fact that the spheres move only a fraction of a lattice constant; during one video frame time (~ 33 ms). Figure 2(b) shows the resulting velocity distributions for several different values of the motor height. The straight-line fit (on these log-linear plots) is the function

$$P(v^2) = Ae^{-mv^2/2kT}$$

from which we can extract the temperature T ; m is the mass of one sphere, k is Boltzmann's constant, and A is a fitting constant. From these distributions we also obtain a calibration curve of temperature vs motor height [Fig. 2(c)].

In the work reported here the system contained 919 spheres, and we easily obtained perfect crystals with a lattice spacing of roughly 8 mm at low T and a capacitor voltage of 2500 V. By slowly lowering the height of the driving motor, we observe the system evolving from a liquid to a solid which is defect-free if the cooling rate is sufficiently low. The presence of the wall potential causes the growth of order to proceed from the surface inward during freezing, as found in computer simulations of systems with solid surfaces. Figure 3 shows time averaged density profiles of the system at various temperatures, clearly showing the persistent ordering at the surface. The temperature at which the central region becomes disordered is distinct, and is taken as defining the boundary between solid and liquid phases, even though the liquid phase retains order very near the walls. The time spent at one temperature is typically twelve hours, the time required to acquire one thousand video frames and reduce them to particle coordinates.

Our study of the two-dimensional melting process has focused on the determination of two order parameters—a translational order parameter η defined as the local

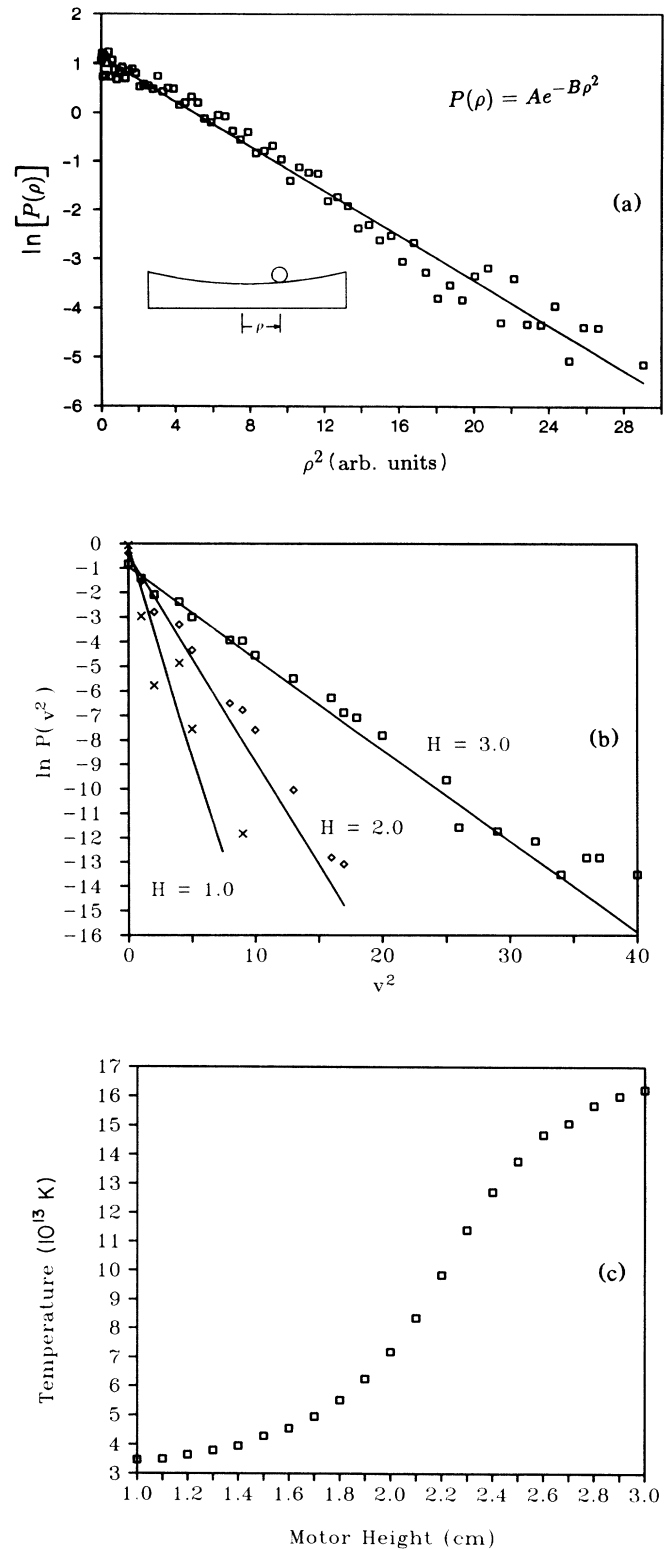


FIG. 2. Temperature calibration: (a) Variation of the radial probability distribution of a single sphere in a parabolic potential produced by a convex lens. The solid line represents the expected Gibbs distribution. (b) Distribution of the square of individual particle velocities in the 919 particle system for three different values of the motor height H . The lines are weighted least-squares fits. (c) Temperature calibration as determined from the velocity distributions of (b).

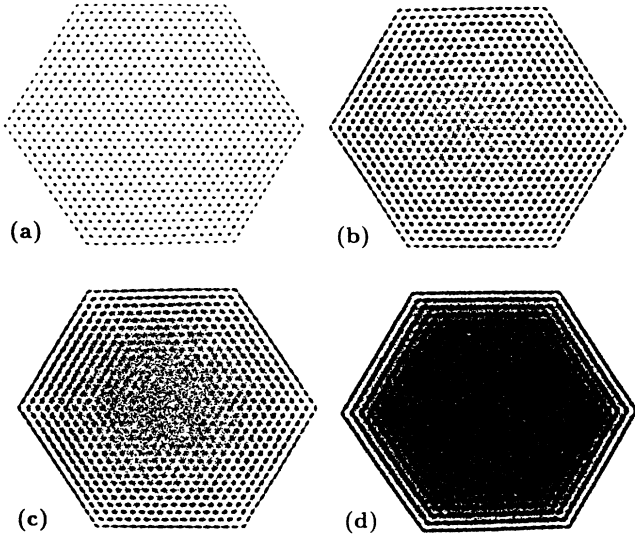


FIG. 3. Density distributions obtained over several hours for (a) the solid phase, (b) at a temperature just below the transition, (c) just after the transition, and (d) in the liquid phase. The strong influence of wall fields forces ordering near the edges of the sample.

Fourier component of the density at a reciprocal lattice vector, and an orientational order parameter η_6 determined by the local sphere-sphere bond angle.

Practically η is defined by

$$\langle \eta \rangle = \frac{1}{N_f} \sum_{j=1}^{N_f} \left| \left\langle \frac{1}{n_j} \sum_{k=1}^{n_j} e^{i\mathbf{G}_0 \cdot \mathbf{r}_k} \right\rangle \right|.$$

The sums are over the number of video frames N_f at a given temperature and the number of particles n_j (typically ~ 300) found in the field of view of frame j . \mathbf{G}_0 is one of the two basis vectors of the reciprocal lattice (calculated from the most ordered phase), and \mathbf{r}_k is the position vector of the k th sphere. The orientational order is characterized by

$$\langle \eta_6 \rangle = \frac{1}{N_f} \sum_{j=1}^{N_f} \frac{1}{n_j} \left| \sum_{p=1}^{n_j} \frac{1}{m_p} \sum_{k=1}^{m_p} e^{i6\theta_{kp}} \right|.$$

Here the sums are over the number of frames N_f , the number of particles n_j in the j th frame, and m_p , the number of nearest neighbors of the p th particle. θ_{kp} is the angle made by the bond between particles k and p . The nearest neighbors were determined by a Voronoi construction.

Figure 4 shows the variation of our order parameters as a function of temperature as well as the height of the driving motor below the sample. It is difficult to discern any two-step mechanism here as the two order parameters appear to increase at the same temperature. According to these observations it is likely that in our system the transition is first order and that the hexatic phase does not exist, in agreement with computer simulations of dipole potentials.^{11–13}

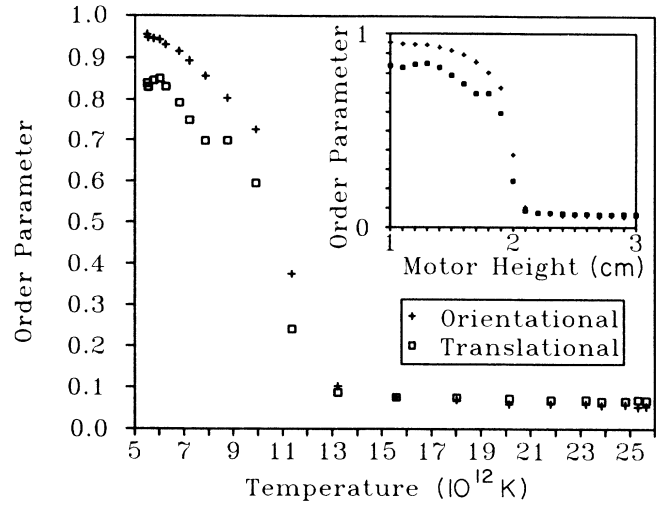


FIG. 4. Variation of translational (boxes) and orientational (crosses) order parameters with temperature; inset shows variation with motor height.

These order parameters differ slightly from the usual indicators of an hexatic phase, namely the long-range behavior of translational and orientational correlation functions.³ We have chosen to determine instead these local measures of translational and orientational order at the cell center partly because our system, like many other experiments and computer simulations, is not large enough to reveal the true long-range behavior of the correlation functions. More importantly, the results of the HNY theory cannot be applied directly to our system due to the presence of an external in-plane field (which is qualitatively different from the kinds of substrate potentials considered by HNY). Modifying the HNY theory by introducing the wall potential $V(\mathbf{r})$ into the Hamiltonian is a formidable task that we have chosen to avoid for the present by contenting ourselves with a qualitative description. If we consider the linear response of an ideal infinite system to our potential $V(\mathbf{r})$, and further make the assumption that this potential does not couple to topological defects, then we can describe the behavior of order parameters in our system in terms of corresponding correlation functions in the $V=0$ system through

$$\langle \eta(\mathbf{r}) \rangle_V = \frac{1}{kT} \langle \eta(\mathbf{r}) \eta(\mathbf{0}) \rangle_0 \otimes V(\mathbf{r}) \quad (1)$$

and similarly for η_6 . The subscripts V and 0 refer to the constrained and unconstrained systems, respectively, and \otimes is a convolution product. The HNY theory predicts that the translational and orientational correlation lengths diverge at different temperatures, resulting, via Eq. (1), in order parameters which go to zero at different temperatures. Such a two-step mechanism should thus be apparent in our measured order parameters, but was not found. Since in known hexatics^{14,15} the system size is comparable to the translational correlation lengths (distances between dislocations), it may be that in our system the large wall forces and relatively small system size combine to suppress the hexatic phase and elevate the solid-

hexatic transition to join the hexatic-liquid transition.

We hope we have conveyed some taste of the possibilities inherent in our model system; it seems ideally suited to studying a variety of topics in statistical mechanics in addition to melting. It is closely related to molecular-dynamics (MD) simulations of classical systems, but with the important advantages of fast (and free) computation time and, at least theoretically, no restrictions on run times or particle number; unlike MD, run times also do not increase with system size. This may be important since some evidence¹⁶ seems to indicate that current MD

run times are insufficiently long to anneal out long-lived topological defects. We also share with MD and colloidal systems the ability to observe the detailed microscopic arrangements and motions of particles, with the added benefit over colloids of having a well-understood interparticle interaction. Our system undergoes a constant volume transition, whereas temperature driven transitions in 2D colloids are difficult.

This work was supported by National Science Foundation Grant No. DMR 88-07443.

*Permanent address: Centre de Recherche Paul-Pascal, 33405 Talence CEDEX, France.

†Permanent address: Cherry Creek High School, Englewood, CO 80111.

¹J. M. Kosterlitz and D. J. Thouless, *J. Phys. C* **6**, 1181 (1973).

²D. R. Nelson, *Phys. Rev. B* **18**, 2318 (1978).

³D. R. Nelson and B. I. Halperin, *Phys. Rev. B* **19**, 2457 (1979).

⁴A. P. Young, *Phys. Rev. B* **19**, 1855 (1979).

⁵K. J. Strandburg, *Rev. Mod. Phys.* **60**, 161 (1988).

⁶C. A. Murray and R. A. Wenk, *Phys. Rev. Lett.* **62**, 1643 (1989); Y. Tang, A. J. Armstrong, R. C. Mockler, and W. J. O'Sullivan, *Phys. Rev. Lett.* **62**, 2401 (1989).

⁷P. Pieranski, J. Malecki, W. Kuczynski, and K. Wojciechowski, *Philos. Mag. A* **37**, 107 (1978).

⁸A. C. Branka and K. W. Wojciechowski, *Mol. Phys.* **56**, 1419

(1985).

⁹A. J. Walton and A. G. Woodruff, *Contemp. Phys.* **10**, 59 (1969).

¹⁰G. E. Blonder, *Bull. Am. Phys. Soc.* **30**, 5403 (1985).

¹¹V. M. Bedanov, G. V. Gadiyak, and Y. E. Lozovik, *Zh. Eksp. Teor. Fiz.* **88**, 1622 (1985) [*Sov. Phys. JETP* **61**, 967 (1985)].

¹²P. Vashishta and R. K. Kalia, in *Melting, Localization, and Chaos*, edited by R. K. Kalia and P. Vashishta (North-Holland, Amsterdam, 1982), p. 43.

¹³R. K. Kalia and P. Vashishta, *J. Phys. C* **14**, L643 (1981).

¹⁴S. B. Dierker and R. Pindak, *Phys. Rev. Lett.* **59**, 1002 (1987).

¹⁵Ming Cheng, John T. Ho, S. W. Hui, and Ronald Pindak, *Phys. Rev. Lett.* **59**, 1112 (1987).

¹⁶A. D. Novaco and P. A. Shea, *Phys. Rev. B* **26**, 284 (1982).

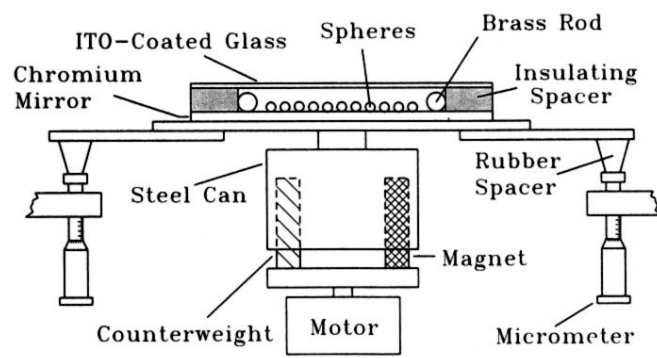


FIG. 1. Diagram of the experimental apparatus.

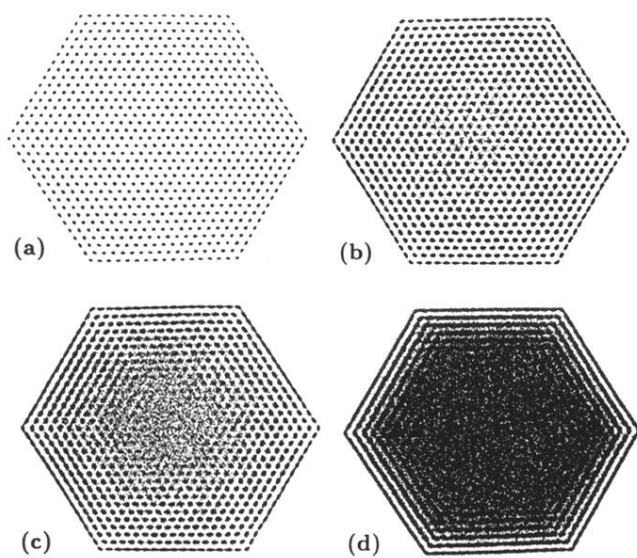


FIG. 3. Density distributions obtained over several hours for (a) the solid phase, (b) at a temperature just below the transition, (c) just after the transition, and (d) in the liquid phase. The strong influence of wall fields forces ordering near the edges of the sample.